We are IntechOpen,
the world's leading publisher of
Open Access books
Built by scientists, for scientists

6,900
Open access books available

186,000
International authors and editors

200M
Downloads

154
Countries delivered to

Our authors are among the

TOP 1%
most cited scientists

12.2%
Contributors from top 500 universities

WEB OF SCIENCE™

Selection of our books indexed in the Book Citation Index
in Web of Science™ Core Collection (BKCI)

Interested in publishing with us?
Contact book.department@intechopen.com

Numbers displayed above are based on latest data collected.
For more information visit www.intechopen.com

Anisotropic Filtering Techniques applied to Fingerprints

Shlomo Greenberg and Daniel Kogan
Ben-Gurion University of the Negev
Israel

1. Introduction

Noise filtering of images is basically a smoothing process, and it is a subject that has been addressed for many years. The idea of adaptive smoothing is being investigated a long time and many different approaches have been proposed over the years.

Mastin (1985) reported superior performance of nonlinear such as medina filtering over linear techniques applied for adaptive image smoothing. Zucker et al. (1977) proposed to perform adaptive smoothing using weighted mask, which is computed by the difference between the value of the center point and its neighbors. Wang et al. (1981) applies a weighting scheme that averages values within a sliding window and changes the weights according to local differential. Instead of basic averaging Davis (Davis & Rozenfeld, 1978) performs iterated local noise cleaning by K-Nearest Neighbour averaging. The main disadvantage of these methods is their difficulty to ensure convergence.

Blake (Blake & Zisserman, 1987) proposed a smoothing process, which reconstructs a noisy signal in a piecewise continuous manner by employing weak continuity constraints. Although the convergence behavior was well studied, the computational complexity is extremely high. An anisotropic diffusion scheme was presented by Perona & Malik (1990). They suggested to employ a heat equation in anisotropic medium for edge enhancement. This is done by selectively smoothing regions with low gradient. Another approach, called Forward-and-Backward diffusion, is presented by Smolka et al. (2003) and emphasizes regions with high gradient which are not caused by noise. Almansa (Almansa & Lindeberg, 2000) and Weickert (2001) have used diffusion techniques, which are based on a multi-scale analysis called scale-space representation, and applied an iterative process for local features estimation. Diffusion methods tend to distort sloping edges, while iterative methods slow down the filtering process in images with considerable amount of noise.

Steerable filters are a class of filters, in which a filter of arbitrary orientation is synthesized as a linear combination of a set of "basis filters" (Freeman & Adelson, 1991). Steerable filters are used in many image-processing tasks and specifically in image enhancement. Steerable-scalable kernels roughly shaped like Gabor functions have the advantage that they can be specified and computed easily (Perona, 1992). However, those filters usually approximate the orientation with low resolution, since they are usually based on angular frequency sampling, and a huge number of basis filters are required in order to approximate orientation steerability with high resolution (Yu et al., 2001). Another kind of structure-

adaptive anisotropic filtering technique has been proposed by Yang et al. (1996). Instead of using local gradients as a means of controlling the anisotropism of filters, it uses both a local intensity orientation and an anisotropic measure to control the shape of the filter. Although the filters proposed by Yang and Almansa are both structure-adaptive anisotropic filters, they are still significantly different mostly by the fact that Almansa's filter is iterative while Yang's is not.

We propose to improve the structure-adaptive anisotropic filter (Yang et al., 1996) in the space domain. We suggest changing the filter's kernel from a circle to an ellipse with the form, size and direction depending on image local anisotropic features. The essential idea of the improved filter is to apply a median filter for pixels bounded by an anisotropic elliptical kernel. We propose to use a non-linear filter kernel function rather than a linear, which produces less blurring during image filtering. The non-linear function is implemented in the form of the median filter. Moreover, instead of using Yang's derivatives-based method for estimation the oriented pattern direction we have used Donahue's (Donahue & Rokhlin, 1993) method, which is more robust to noise. It uses a gradient type local operator and least squares minimization to control the noise.

Fingerprints are today the biometric features most widely used for personal identification. The uniqueness of a fingerprint is determined by the local ridge characteristics and their relationships. Most of today's automatic systems used for fingerprint comparison are based on minutiae matching, which represents local discontinuities in a fingerprint image. An automatic fingerprint image matching process, which enables a personal identification, strongly depends on comparison of the minutiae points of interest MPOI and their relationships. Reliable automatic extraction of these MPOI is a critical step in fingerprint classification. The performance of minutiae extraction algorithm relies heavily on the quality of the fingerprint images (Hong et al., 1996). The ridge structures in poor-quality fingerprint images are not always well defined and, hence, cannot be correctly detected. In order to ensure robust performance of minutiae extraction algorithm an enhancement algorithm that improves the clarity of the ridge structures is necessary (Hong et al., 1996). Enhancement of ridge structures essentially involves some filtering operation.

We propose to modify the structure-adaptive anisotropic filter in the frequency domain by converting it from a lowpass filter into a band-pass one. In this work we show that the modified structure-adaptive anisotropic filter can be effectively applied to applications, such as fingerprint image enhancement, in which the oriented patterns in local neighborhood form a sinusoidal-shaped plane wave with a welldefined frequency and orientation i.e., ridges and valleys in a fingerprint image. Adjustment of the modified filter to fingerprints is made resulting in a unique structure-adaptive anisotropic filter. The performance of the unique structure-adaptive anisotropic filter is compared to that of some other filters in the framework of minutiae detection process.

2. The structure-adaptive anisotropic filter

The structure-adaptive anisotropic filter, which has been proposed by Yang, uses a local intensity orientation and an anisotropic measure of level contours to control the shape and extent of the filter kernel. The filter kernel applied at each point x_0 is defined as follows (Yang et al., 1996):

$$k(x_0, x) = \rho(x - x_0) \exp\left\{-\left[\frac{((x-x_0) \cdot n)^2}{\sigma_1^2(x_0)} + \frac{((x-x_0) \cdot n_\perp)^2}{\sigma_2^2(x_0)}\right]\right\} \tag{1}$$

where n and $n_\perp$ are mutually normal unit vectors, and n is parallel with the local oriented pattern direction. The shape of the kernel is controlled through $\sigma_1^2(x_0)$ and $\sigma_2^2(x_0)$, ρ satisfy the condition $\rho(x) = 1$ when $|x| < r$, and r is the maximum support radius.

Direction estimation of an oriented pattern is based on the fact that the power spectrum of such a pattern lies along a line through the origin in the Fourier domain, and the direction of the line is perpendicular to the dominant spatial orientation of the pattern. The evaluation of the Fourier transform, however, is not necessary for actual calculations. Through a simple relationship between the local orientation direction and the matrix eigenvectors, the estimation of oriented pattern direction $\theta(x)$ [the direction of vector n in (1)] can be made (Yang et al., 1996) as follows:

$$\theta(x) = \frac{1}{2} \tan^{-1}\left\{\frac{\iint_\Omega 2 \cdot \left(\frac{\partial f}{\partial x_1}\right)\left(\frac{\partial f}{\partial x_2}\right) dx_1 dx_2}{\iint_\Omega \left(\frac{\partial f}{\partial x_1}\right)^2 - \left(\frac{\partial f}{\partial x_2}\right)^2 dx_1 dx_2}\right\} + \frac{\pi}{2} \tag{2}$$

where Ω is a local neighborhood $x = (x_1, x_2)$.

The space constants $\sigma_1^2(x_0)$ and $\sigma_2^2(x_0)$ are controlled through the corner detector $c(x_0)$ and by the measurement of anisotropism $g(x_0)$ as follows (Yang et al., 1996):

$$\sigma_1(x_0) = \frac{r}{1 + c(x_0)/\beta} \tag{3}$$

$$\sigma_2(x_0) = (1 - g(x_0))\frac{r}{1 + c(x_0)/\beta} \tag{4}$$

where β is a normalization factor that controls how faithfully the corners and junctions can be preserved during the filtering process.

The anisotropic measure gives an indication of how strong a pattern is oriented and is defined as follows (Yang et al., 1996):

$$g(x) = \frac{\left\{\iint_\Omega \left(\frac{\partial f}{\partial x_1}\right)^2 - \left(\frac{\partial f}{\partial x_2}\right)^2 dx_1 dx_2\right\}^2 + \left\{\iint_\Omega 2\cdot\left(\frac{\partial f}{\partial x_1}\right)\left(\frac{\partial f}{\partial x_2}\right) dx_1 dx_2\right\}^2}{\left\{\iint_\Omega \left(\frac{\partial f}{\partial x_1}\right)^2 + \left(\frac{\partial f}{\partial x_2}\right)^2 dx_1 dx_2\right\}^2} \tag{5}$$

which can be calculated directly from the original data $f(x_1, x_2)$ and its partial derivatives.

The anisotropic measure can also provide a convenient way of finding corner and junction points within a given image. Yang suggests using both the measure of anisotropism and a gradient strength for an estimation of corner strength in a following way (Yang et al., 1996):

$$c(x) = (1 - g(x))|\nabla f(x)|^2 \tag{6}$$

3. Improved structure-adaptive anisotropic filter

In this section we propose some improvements to the structure-adaptive anisotropic filter (Yang et al., 1996) in the space domain. As previously mentioned the essential idea of the improvement is to apply the median filter for pixels bounded by an anisotropic elliptical kernel.

The structure-adaptive anisotropic filter suffers from the following problems: corner strength measure $c(x)$ is highly influenced by noise. This results in a wrong estimation of space constants $\sigma_1^2(x_0)$ and $\sigma_2^2(x_0)$, which control the shape of the filter kernel. Derivatives-based approach for oriented pattern direction estimation fails to produce correct estimates for noisy images. The normalization factor β controls how faithfully the corners and junctions can be preserved during the filtering process. Therefore, it is a critical factor and the choise of β significantly affects the filter performance. Despite the fact that the structure-adaptive filter is directional and adjusts the shape of the kernel according to image anisotropic local features, the filter causes to unnecessary blurring in processed image due the linearity of its filtering function. The structure-adaptive anisotropic filter operates on a pixels neighborhood of a constant size and moreover, the size is not depending on local features of input image. We suggest a solution to the above-mentioned problems and propose the improved structure-adaptive anisotropic filter, which combines non-linear filtering function, a more robust to noise technique for oriented pattern direction estimation and elliptical kernel with its form, size and direction depending on image local anisotropic features.

Instead of using a constant kernel the size must be changed to embody image local anisotropic features, namely, the anisotropic measure $g(x)$ and the corner strength $c(x)$. This can be achieved by defining an elliptical kernel (Fig. 1) with its principal axis and direction changing according to image local anisotropic features.
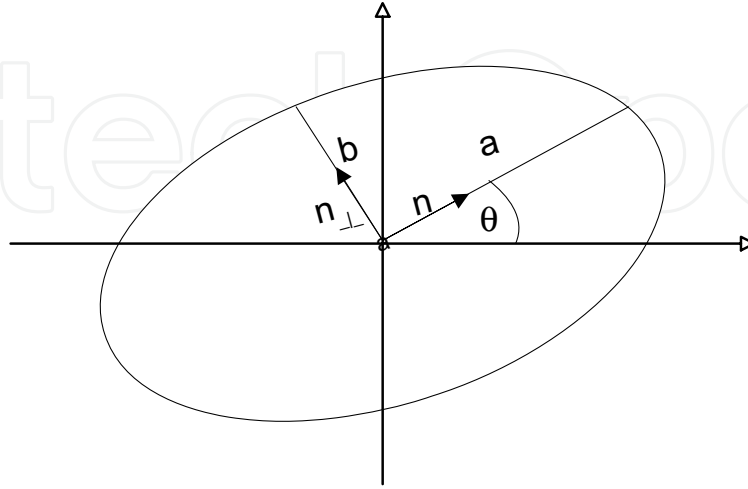
Fig. 1. Controlling the shape and direction of an elliptic kernel through principal axes a, b and direction θ, which are controlled through image local anisotropic features.

The elliptical kernel's main axis $a(x_0)$ must be minimal in regions where there is a high number of corners (edges, corners and etc) and maximal in regions with no corners (smooth places). The transition of $a(x_0)$ from smooth regions to regions that include corners should be performed in an exponential manner in order to prevent smoothing corners. The kernel's shape must be circular in regions with low values of anisotropic measure ($g \rightarrow 0$). In regions with high anisotropic measure ($g \rightarrow 1$) the shape obtains a highly oriented elliptical form with its main axis runs in parallel to direction of local oriented pattern as can be seen in Fig. 2. To meet these requirements we propose to define the principal axes of the elliptical kernel as follows:

$$a(x_0) = r \cdot \exp\left(\frac{-c(x_0)}{\beta}\right) \tag{7}$$

$$b(x_0) = a(x_0) \cdot \left(1 - g(x_0) + \varepsilon\right) \tag{8}$$

where r is the maximal support radius, ε is the minimal kernel width and β is a normalization factor that will be defined later.

Comparing the behavior of Yang's space parameter $\sigma_1(x_0)$ (3) with the new proposed $a(x_0)$ parameter (7) emphasis the improvement of the new filter. Fig. 3 demonstrates the behavior of controlling the main axis of the filter kernel for both Yang's and the proposed filter. This figure shows that adopting the proposed filter results with better behavior relative to the corner strength $c(x)$. For high values of corner strength the elliptical kernel results with smaller values for the main axis $a(x_0)$ in comparison to Yang's filter, and only few pixels

are collected by the kernel. Therefore, it suggests that the improved filter better preserves corners and edges in the input image.
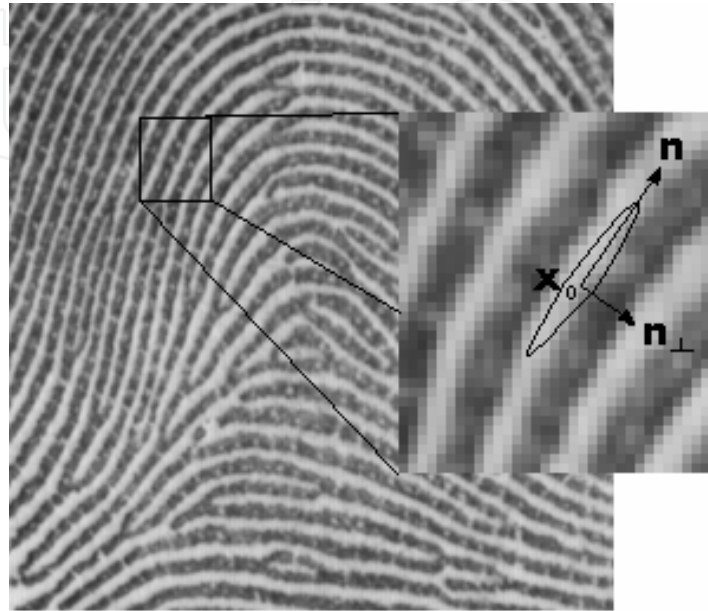

Fig. 2. Controlling the shape and direction of the kernel in the space domain.
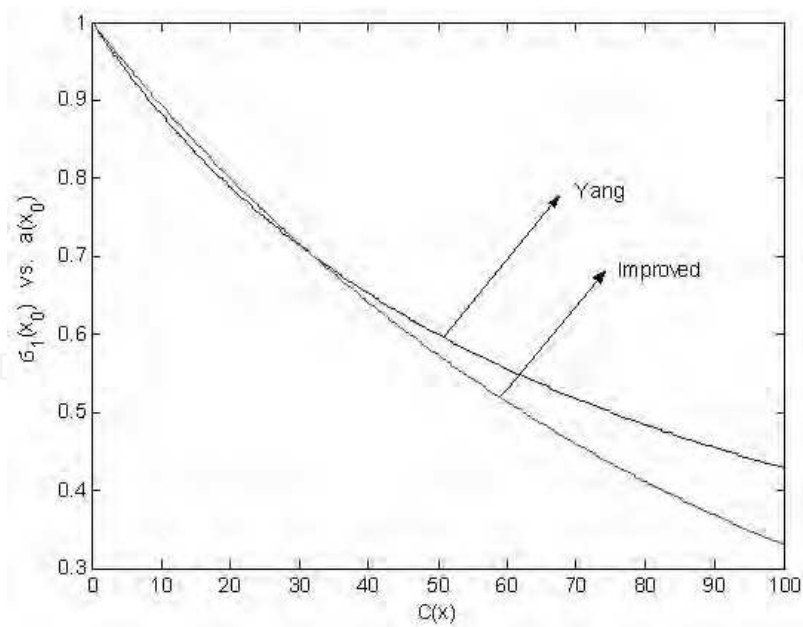

Fig. 3. Controlling the main axis of the filter kernel for Yang's and the improved filter.

Correct estimation of oriented patterns direction is of high importance for effective performance of directional filters such as structure-adaptive anisotropic filter. The technique, which was proposed by Yang, is based on the fact that the power spectrum of an oriented pattern lies along a line through the origin in the Fourier domain, and the direction of the line is perpendicular to the dominant spatial orientation of the pattern. This technique fails to produce correct estimates for noisy images. The proposed filter adopts the method, proposed by Donahue & Rokhlin (1993), which uses a gradient-type operator and least-squares minimization to control the noise. The estimation of the oriented pattern direction is extracted from each $2x2$ pixels neighborhood, which is then averaged over a local window of 5x5 pixel size.

We propose to use a non-linear filter kernel function rather than a linear one that produces less blurring during image filtering. We have implemented the non-linear function in the form of a median filter that is applied within neighborhoods of pixels bounded by an elliptical kernel. The obtained is the improved structure-adaptive anisotropic filter, which is expressed mathematically as follows:

$$k(x_0, x) = median\{f(x), \ x \in P(x - x_0)\} \tag{9}$$

where $P(x - x_0)$ is the elliptical kernel centered at pixel x_0, oriented at angle θ (defined by mutually normal unit vectors n and $n_\perp$) and is defined as follows:

$$\frac{((x_1 - x_{01}) \cdot n)^2}{a(x_0)^2} + \frac{((x_2 - x_{02}) \cdot n_\perp)^2}{b(x_0)^2} \leq 1 \tag{10}$$

Substituting (7) and (8) into (10) and incorporating the obtained equation into (9) results in a final expression of improved structure-adaptive anisotropic filter:

$$k(x_0, x) = median\left\{ f(x), \ x \in \left(\frac{((x_1 - x_{01}) \cdot n)^2}{\left(r \cdot \exp\left\{ \frac{-c(x_0)}{\beta} \right\} \right)^2} + \frac{((x_2 - x_{02}) \cdot n_\perp)^2}{\left(r \cdot \exp\left\{ \frac{-c(x_0)}{\beta} \right\} \cdot (1 - g(x_0) + \varepsilon) \right)^2} \leq 1 \right) \right\} \tag{11}$$

Normalization factor β used in the structure-adaptive anisotropic filter (Yang (1996)) is set to 75 percent of the maximal value of $c(x)$. Appropriate choice of β involves a trade off between effective smoothing of areas with no corners (higher β) and preserving most of the corners in the image (setting lower β). Fig. 4 shows the PSNR of a reconstructed image using different β values. Fig. 4 suggests using higher values of β to obtain higher PSNR

values for the reconstructed image. However, Fig. 5 which demonstrates the reconstructed image, shows that the image is over smoothed while using high value of β. Therefore, in order to preserve most of the corners and to effectively smooth areas without corners, we suggest setting β to 90 percent of the maximal value of $c(x)$. This compromise is empirically achieved by testing different values for β.

The performance of the improved structure-adaptive anisotropic filter is compared to the structure-adaptive anisotropic filter (Yang, 1996) and to the conventional median filter. The conventional median filter is carried out by numerical sorting of all pixel values in a surrounding neighborhood of 3x3 pixels, and then replacing the pixel being considered with the middle pixel value.

The maximal support radius used for the structure-adaptive anisotropic filter is 3 pixels as suggested by Yang (1996), while the maximal support radius for the improved structure-adaptive filter was empirically set to 2 pixels. The comparison is carried out on different kinds of images, which are commonly used for testing noise filtering algorithms (Fig.). All the test images are of resolution 79x79 dots per inch. The size is 182x144 for Bird image, 95x95 for Girl and Area images, and 256x256 pixels for Fingerprint image.
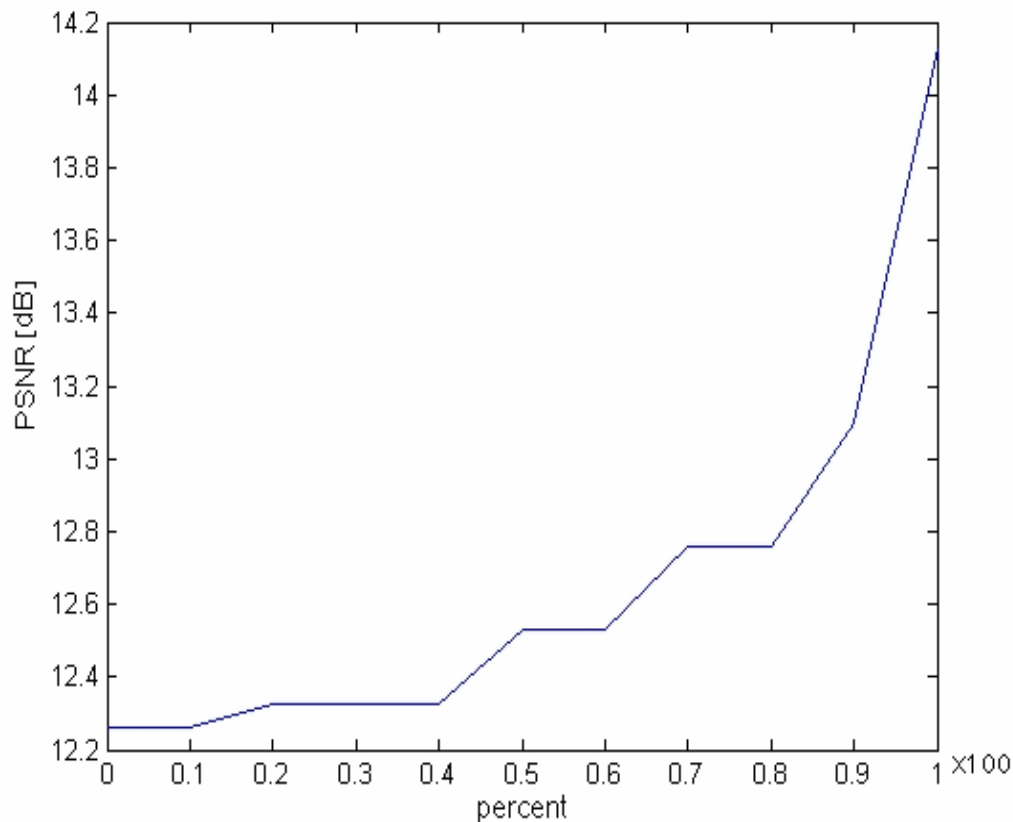

Fig. 4. PSNR of reconstructed Bird image using different β

(a)   (b)   (c)   (d)

Fig. 5. Result of applying the improved filter with different β : (a) 50%, (b) 75%, (c) 90% and (d) 100% of the maximal value of $c(x)$.

(a)   (b)   (c)   (d)

Fig. 6. Test images: (a) Bird ,(b) Girl (c) Area and (d) Fingerprint image

The filters were tested on images contaminated by Gaussian noise and 'Salt and Pepper' noise for different SNR (Signal to Noise) levels. Figure 7 demonstrates the Bird image contaminated with 'Salt and Pepper' noise and Gaussian noise.

(a)   (b)   (c)
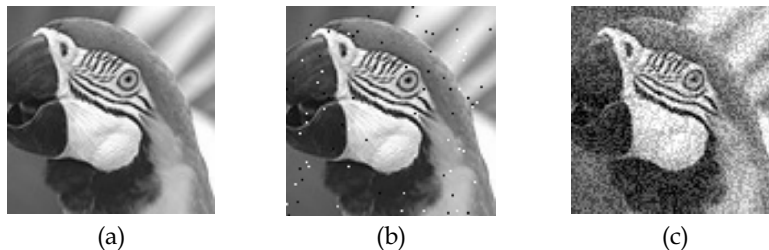
Fig. 7. (a) original Bird image, contaminated with (b) 'Salt and Pepper' noise with SNR=21dB, and (c) Gaussian noise with SNR=20dB.

The performance comparison is based on the SAD (Sum of Absolute Differences) criteria, which computes the sum of absolute differences between the original image and the reconstructed one. Figure 8 shows the filters performance results for Gaussian noise for different levels of SNR ranging from 15dB to 80dB. Figure 9 shows the performance results for 'Salt and Pepper' noise for different levels of SNR ranging from 16dB to 52dB. Yang's structure-adaptive anisotropic filter performs better than the median filter. The improved structure-adaptive anisotropic filter outperforms both median and Yang's structure-adaptive anisotropic filter over the whole range of SNR levels. Figure 10 shows some examples of applying the different filters on images contaminated by Gaussian noise. It can be seen that the Yang's structure-adaptive anisotropic filter reconstructs better than the

median filter, and the improved structure-adaptive anisotropic filter outperforms both filters in reconstructing from noisy image.
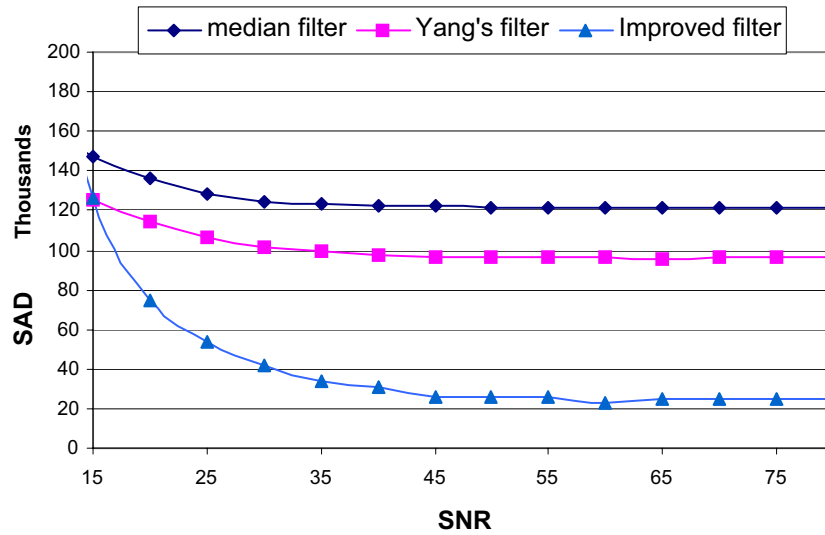

Fig. 8. Performance results of applying a conventional median filter, Yang's structure-adaptive anisotropic and the improved structure-adaptive anisotropic filters on the Bird image contaminated by a Gaussian noise at different SNR levels.
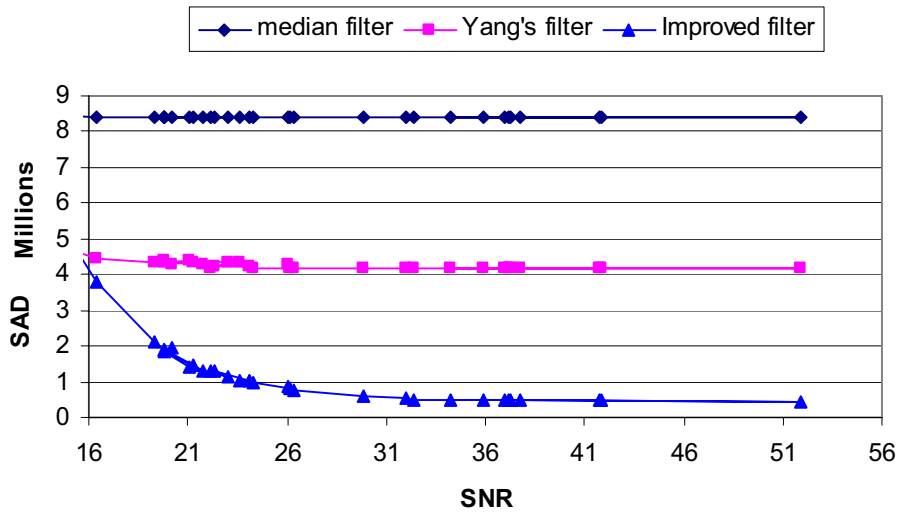

Fig. 9. Performance results of applying a conventional median filter, Yang's structure-adaptive anisotropic and the improved structure-adaptive anisotropic filters on the Bird image contaminated by a 'Salt and Pepper' noise at different SNR levels.
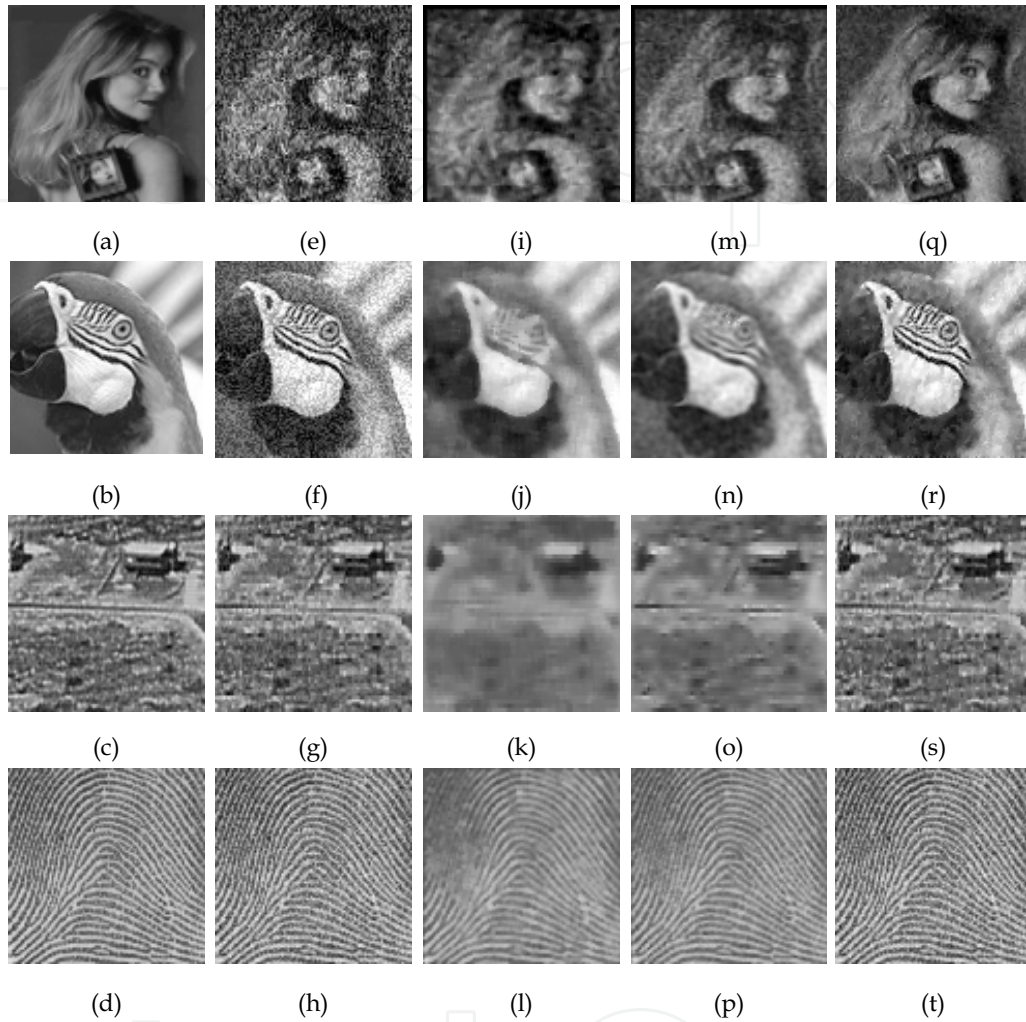
Fig. 10. Applying the different filters on images contaminated by Gaussian noise: Original images (a)-(d), with Gaussian noise (SNR:10dB) (e) and (SNR:20dB) (f)-(h), images reconstructed by the median filter(i)-(l), by the structure-adaptive anisotropic filter(m)-(p) and by the proposed improved structure-adaptive anisotropic filter (q)-(t).

4. The modified structure-adaptive anisotropic filter

In this section we propose some modifications to the structure-adaptive anisotropic filter (Yang et al., 1996) in the frequency domain and present the modified structure-adaptive anisotropic filter.

The structure-adaptive filter has the low-pass filter characteristics. We propose to convert it to the band-pass filter by multiplying its kernel by a scaling factor S and adding an offset V.

The obtained is the modified structure-adaptive anisotropic filter, which has the following general form:

$$h(x_0, x) = V + S \cdot \rho\,(x - x_0) \exp\left\{ -\left[\frac{((x - x_0) \cdot n)^2}{\sigma_1^{\,2}(x_0)} + \frac{((x - x_0) \cdot n_\perp)^2}{\sigma_2^{\,2}(x_0)} \right] \right\} \tag{12}$$

where V and S are the parameters, which must be adjusted to the specific application. Applying a 2D Fourier transform on (12) we obtain the filter's frequency response:

$$H(u, v) = V \cdot 4\pi^2 \delta(u, v) + \frac{1}{\pi\beta} S\left(\frac{\sin(ur)}{u} * \exp\left\{ -\frac{u^2}{4\beta} \right\} \right) \cdot \left(\frac{\sin(vr)}{v} * \exp\left\{ -\frac{v^2}{4\beta} \right\} \right)$$

$$\beta = \left(\frac{\cos\theta}{\sigma_1(x_0)} \right)^2 + \left(\frac{\sin\theta}{\sigma_2(x_0)} \right)^2 \tag{13}$$

where θ is the local pattern orientation, r is the kernel's maximal support radius and $*$ is a convolution operator.

The general form of the modified structure-adaptive anisotropic filter can obtain different frequency response behavior types (low-pass and band-pass) by matching the values of V and S (Figure 6). The structure-adaptive filter (Yang et al., 1996) can be seen as a special case of the modified structure-adaptive anisotropic filter and it is obtained by setting the values to S=1 and V=0.
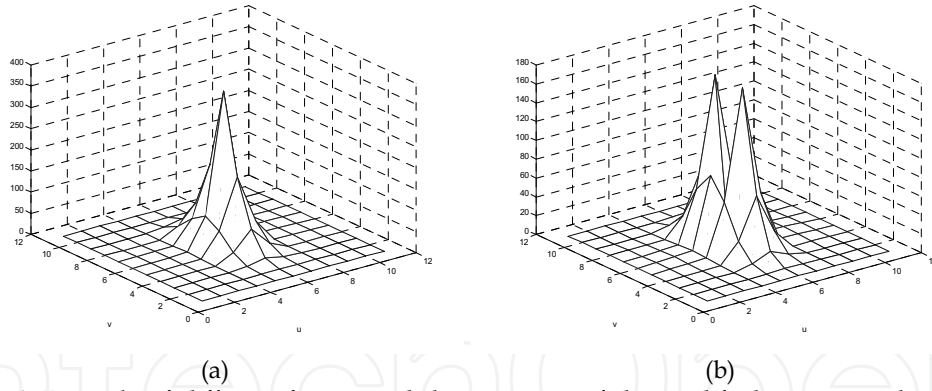

(a)   (b)

Fig. 6. Example of different frequency behavior types of the modified structure-adaptive anisotropic filter :(a) low-pass filter type (V=1 S=10) and (b) band-pass filter type (V=-2 S=10)

Band-pass form of the modified structure-adaptive anisotropic filter is effective in filtering images in which oriented patterns in a local neighborhood form a sinusoidal-shaped plane wave with a well-defined frequency and orientation (i.e. fingerprint images including ridges and valleys).

5. The unique structure-adaptive anisotropic

In this Section the application of the modified structure-adaptive anisotropic filter to fingerprint image enhancement is made and the unique structure-adaptive anisotropic filter is proposed. Fingerprints are today the biometric features most widely used for personal identification. Fingerprint recognition is one of the basic tasks of the Integrated Automated Fingerprint Identification Service (IAFIS) of the most famous police agencies (Lee & Gaensslen, 1991). A fingerprint pattern is characterized by a set of ridgelines that often flow parallel, but intersect and terminate at some points. The uniqueness of a fingerprint is determined by the local ridge characteristics and their relationships (Hong et al., 1998), (Lee & Gaensslen, 1991). Most automatic systems for fingerprint comparison are based on minutiae matching (Hollingum, 1992). Minutiae characteristics are local discontinuities in the fingerprint pattern and represent the two most prominent local ridge characteristics: terminations and bifurcations A ridge termination is defined as the point where a ridge ends abruptly, while ridge bifurcation is defined as the point where a ridge forks or diverges into branch ridges (Figure 7). A typical fingerprint image contains about 40-100 minutiae (Hong et al., 1998).
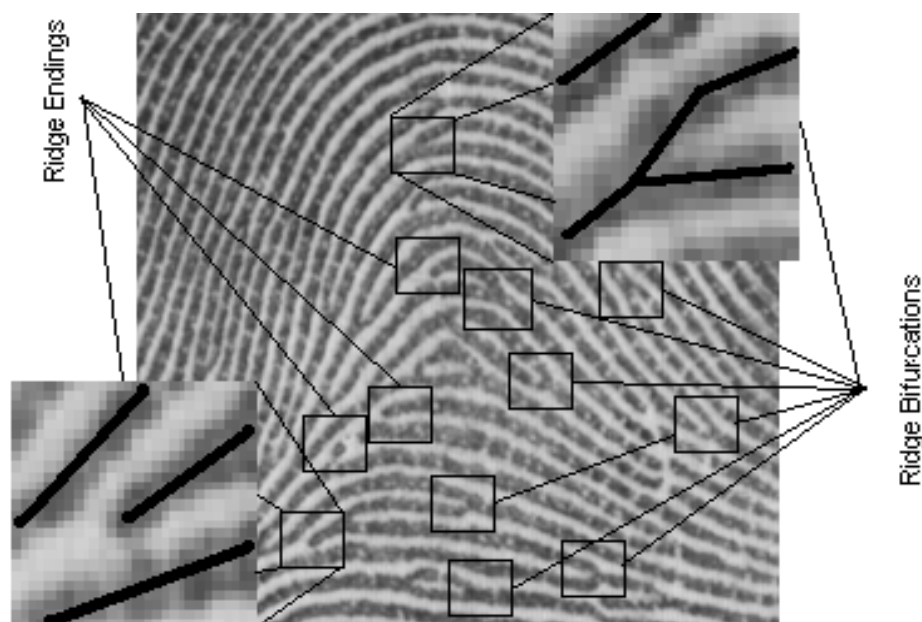

Fig. 7. Examples of minutiae (ridge ending and bifurcation) in a fingerprint image

An automatic fingerprint image matching process, which enables a personal identification, strongly depends on comparison of the Minutiae Points of Interest (MPOI) and their relationships. Reliable automatic extraction of these MPOI is a critical step in fingerprint classification.

The performance of minutiae extraction algorithm relies heavily on the quality of the fingerprint images (Hong et al., 1998). The ridge structures in poor-quality fingerprint images are not always well defined and, hence, cannot be correctly detected. This might result in the creation of spurious minutiae and the ignoring of genuine minutiae. Therefore

large errors in minutiae localization may be introduced (Hong et al., 1998). Examples of poor-quality fingerprint images are shown in Figure 8. In order to ensure robust performance of minutiae extraction algorithm an enhancement algorithm that improves the clarity of the ridge structures is necessary (Hong et al., 1998), (Hong et al., 1996).

Most of the fingerprint image enhancement techniques, proposed in the literature, are applied to binary images, while some others operate directly on gray-scale images (Lee & Gaensslen, 1991), (O'Gorman, L. & Nickerson, 1989), (Sherlock et al., 1994). The binarization process may cause loss of information about true ridge structure and it has inherent limitations (Hong et al., 1998).

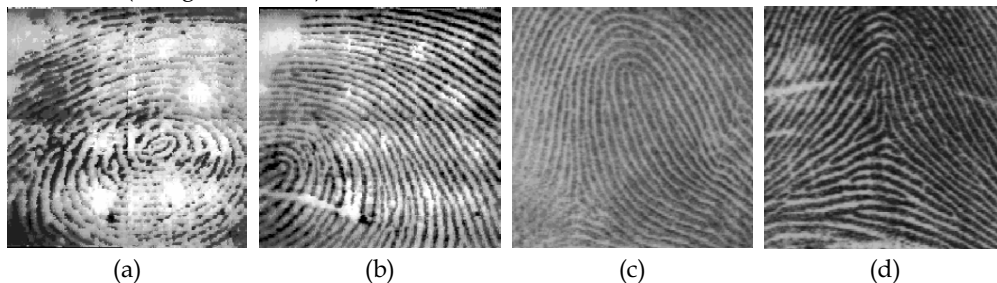(a)   (b)   (c)   (d)

Fig. 8. Examples of poor quality fingerprint images due to: noisy acquisition device (a), (b) and variation in impression conditions (c), (d), resulting in corrupted ridgelines

Ko (2002) and Sherlock et al. (1994) suggested gray-scale image enhancement techniques, which are applied in the frequency domain, while Hong et al. (1998) and Huvanandana et al. (2003) employed their techniques directly in the space domain. Cheng et al. (2002) applies scale space theory to fingerprints enhancement by filtering the image in an iterative manner using both local and global image characckteristics. Almansa & Lindeberg (2000) propose a diffusion technique, which estimates iteratively local features and perfoms directional filtering in regions with well-defined orientation, while in areas without a dominant orientation it applies isotropic filtering. Wang & Wang (2004) propose similar technique, which applies isotropic filtering in the frequency domain at regions without clear dominant orientation.

Different gray-scale fingerprint images enhancement techniques assume that the local ridge frequency and orientation can be reliably estimated. However, this assumption is not valid for poor-quality fingerprint images. Although, other decomposition methods (Hong et al., 1998), (Hong et al., 1996) which apply a bank of Gabor filters to the input fingerprint images, can obtain reliable orientation estimation even for corrupted images, they are computationally expensive.

Hong et al. (1998) proposed a fast enhancement algorithm, which can adaptively improve the clarity of ridge and valley structures of input fingerprint images based on the estimated local ridge orientation and frequency.

We present some improvement to the Hong (Hong et al., 1998) method by using the modified structure-adaptive anisotropic filter, adapted to fingerprint images. Instead of using both local ridge orientation and local frequency information, only the orientation information is used in our approach. Our proposed unique structure-adaptive anisotropic filter, which eliminates the need to estimate local frequency information, can replace the Gabor filter. The proposed enhancement algorithm with the unique filter is faster and efficient as well.

We have adjusted the modified structure-adaptive anisotropic filter specifically to fit fingerprint images, and empirically set the filter parameters to $V = -2$ and $S = 10$. The filter frequency response has bandpass filter characteristics. The proposed filter was found to be effective in fingerprint image enhancement, while preserving the local ridge frequency of the fingerprint image (see Figure 10). The frequency bands transferred by the filter include almost all typical local ridge frequencies that lie within a certain range for a given image resolution (Hong et al., 1998).

The space constants $\sigma_1^2(x_0)$ and $\sigma_2^2(x_0)$ of the structure-adaptive anisotropic filter kernel are controlled through both the corner detector $c(x)$ and by the measurement of anisotropism $g(x)$ as defined by (5) and (6). These equations include gradient estimation via calculations of first order derivatives of the input image. Problems may arise if the input data is noisy. This is because taking derivatives is a highpass filtering process, which amplifies the effect of noise. The space constants have a strong influence on filter performance on fingerprint images, and since they are highly affected by noise, we suggest setting them to constants $\sigma_1^2(x_0) = 4$ and $\sigma_2^2(x_0) = 2$. This setting produced a filter in the form of a Gaussian-shaped kernel with a double ratio between the axis running in the main direction and the axis perpendicular to it. By setting the space constants to constant values we obtain a filter that is more robust to noise. However, the filter is optimal only for a fingerprint set, which was used in our experiments. Therefore in our future work we will develop more robust to noise local anisotropic measurements that will control the space constants. Figure 9 shows a comparison of impulse and frequency responses between the structure-adaptive anisotropic filter (Yang et al., 1996) and the unique filter ($V = -2$, $S = 10$). It can be seen that both filters have directional Gaussian-like shaped kernels in a space domain. However, they are different in the frequency domain: the Yang's anisotropic filter shows Low-Pass (one peak in the center) filter characteristics, while the unique anisotropic filter expresses Band-Pass filter characteristics (two peaks symmetrically located around the center).

The unique filter has one undesired property: its value at infinity is unequal to zero. Therefore its response depends on the chosen support size of the filter. However, the unique filter is adjusted to transfer all typical local ridge frequencies, which lie within a certain range for a given image resolution (Hong et al., 1998), and it works well on all set of fingerprint images with given resolution, as demonstrated in the next Section.

The performance of the unique structure-adaptive anisotropic filter is studied in the context of fingerprint image enhancement algorithm simulated by Hong (1998). We compare the applying of the structure-adaptive anisotropic filter J (Yang, 1996), the unique structure-adaptive anisotropic filter I, Gabor-based filter G (Hong, 1998) and the modified Gabor-based filter (Greenberg et al., 2000 & Greenberg et al., 2002) H, on the same set of fingerprint images. We use performance results of the structure-adaptive anisotropic filter I and Gabor filters G, H taken from a different comparative study (Greenberg et al., 2000 & Greenberg et al., 2002) conducted on direct gray-scale fingerprint enhancement methods. In this work we extend this comparative study with performance results of the unique structure-adaptive anisotropic filter J applied on the same fingerprint images set as in (Greenberg et al., 2000 & Greenberg et al., 2002). The sample set is composed of 10 fingerprints taken from NIST, FBI sample and using an optoelectronic device. The gradient used by compared filtering algorithms was obtained using first order approximation.

Figure 10 shows a comparison of the enhancement results obtained using different filters, for poor-quality fingerprint images, which contain regions that do not form a well-defined local ridge frequency. These regions are mostly encountered in the neighbourhood of fingerprint image singular points: core and delta (Lee & Gaensslen, 1991). Both the structure-adaptive and the unique structure-adaptive anisotropic filters outperform the Gabor-based filters for those regions, which contain singular points.
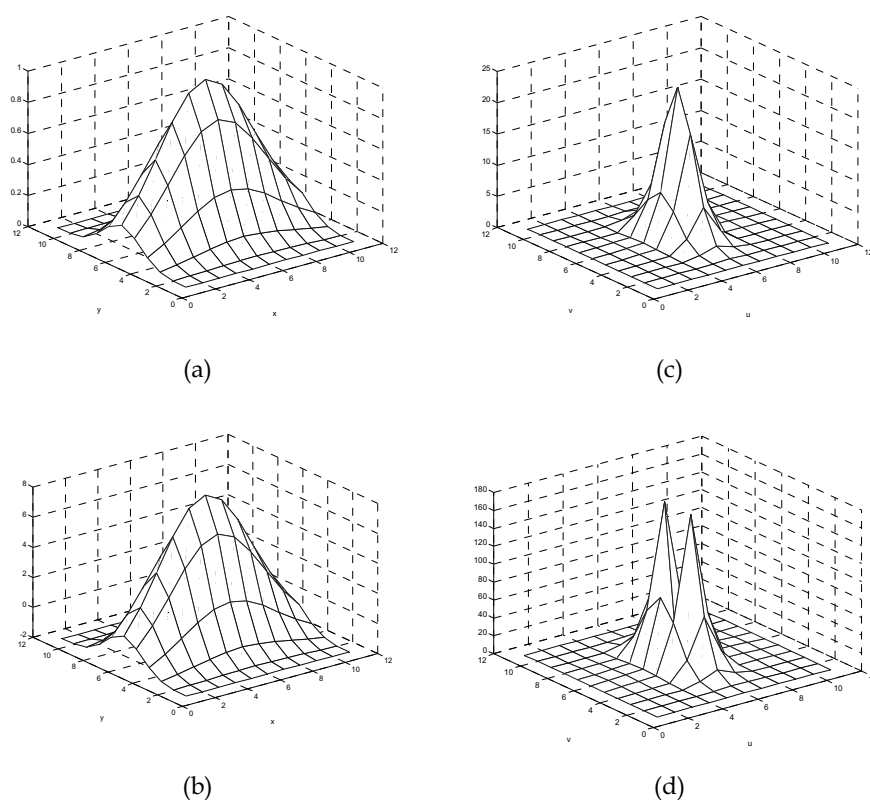

(a)   (c)

(b)   (d)

Fig. 9. Comparison of impulse and frequency response between the structure-adaptive anisotropic filter and the proposed unique structure-adaptive anisotropic filter ($V = -2$, $S = 10$). Both filters are 11x11 pixels kernel size, and have a directional Gaussian-like shaped kernel in a space domain (a) and (b). However they are different in the frequency domain: (c) the structure-adaptive anisotropic filter shows lowpass filter characteristics, while (d) the unique filter expresses bandpass filter characteristics (two peaks around the center).

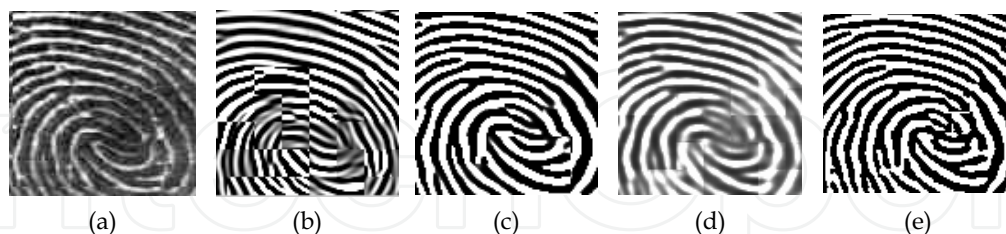(a)   (b)   (c)   (d)   (e)

Fig. 10. Example of enhancement results of fingerprint image region with a singular point (core). Original image (a); enhanced image after applying the Gabor-based filter (b), the modified Gabor-based filter(c), the structure-adaptive anisotropic filter (d) and the proposed unique structure-adaptive anisotropic filter (e)

Figure 11 compares the success rate obtained by applying gray-scale filtering technique (Greenberg et al., 2000 & Greenberg et al., 2002) using the four filters (G, H, I, J) on the same fingerprint image set. The average error percentage is expressed in terms of false (minutiae that was found in the region not containing true minutiae), dropped (minutiae that was not found in the neighborhood of true minutiae) and exchanged minutiae (minutiae differing from the true minutiae type in the same image region). The average error percentage presented by our approach I (unique structure-adaptive anisotropic filter), is comparable to the errors produced by approach H (modified Gabor-based filter). Both I filter and H filter create less errors than the G (Gabor-based) and I (structure-adaptive anisotropic) filters.
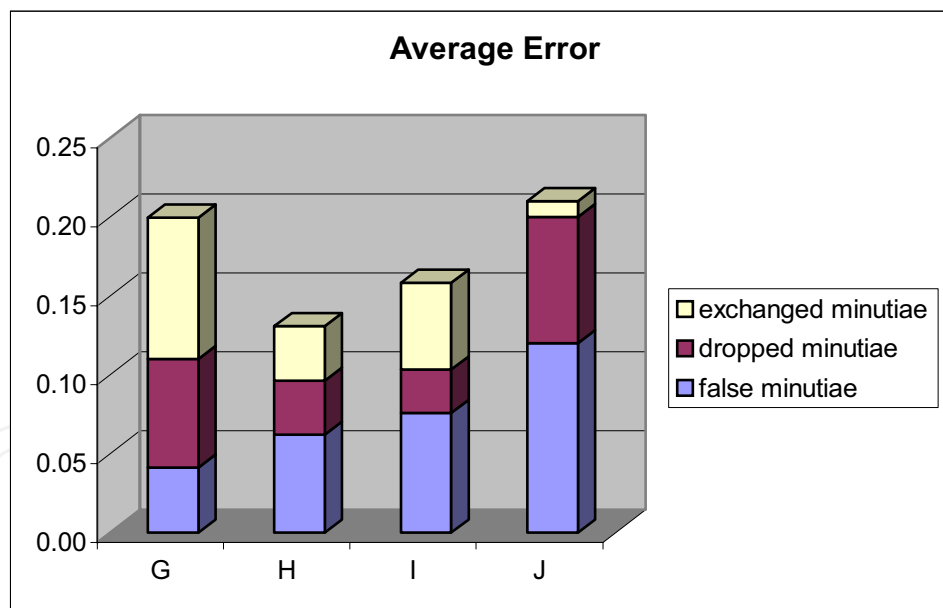

Fig. 11. Comparison of the filters performance: G-Gabor-based filter, H-modified Gabor–based filter, I-unique proposed structure-adaptive anisotropic filter and J-structure-adaptive anisotropic filter.

Figure 10 demonstrates the enhancement results of applying the structure-adaptive anisotropic (Yang, 1996), the unique structure-adaptive anisotropic and the modified Gabor-based (Greenberg et al., 2000 & Greenberg et al., 2002) filters to some fingerprint images from the sample set.
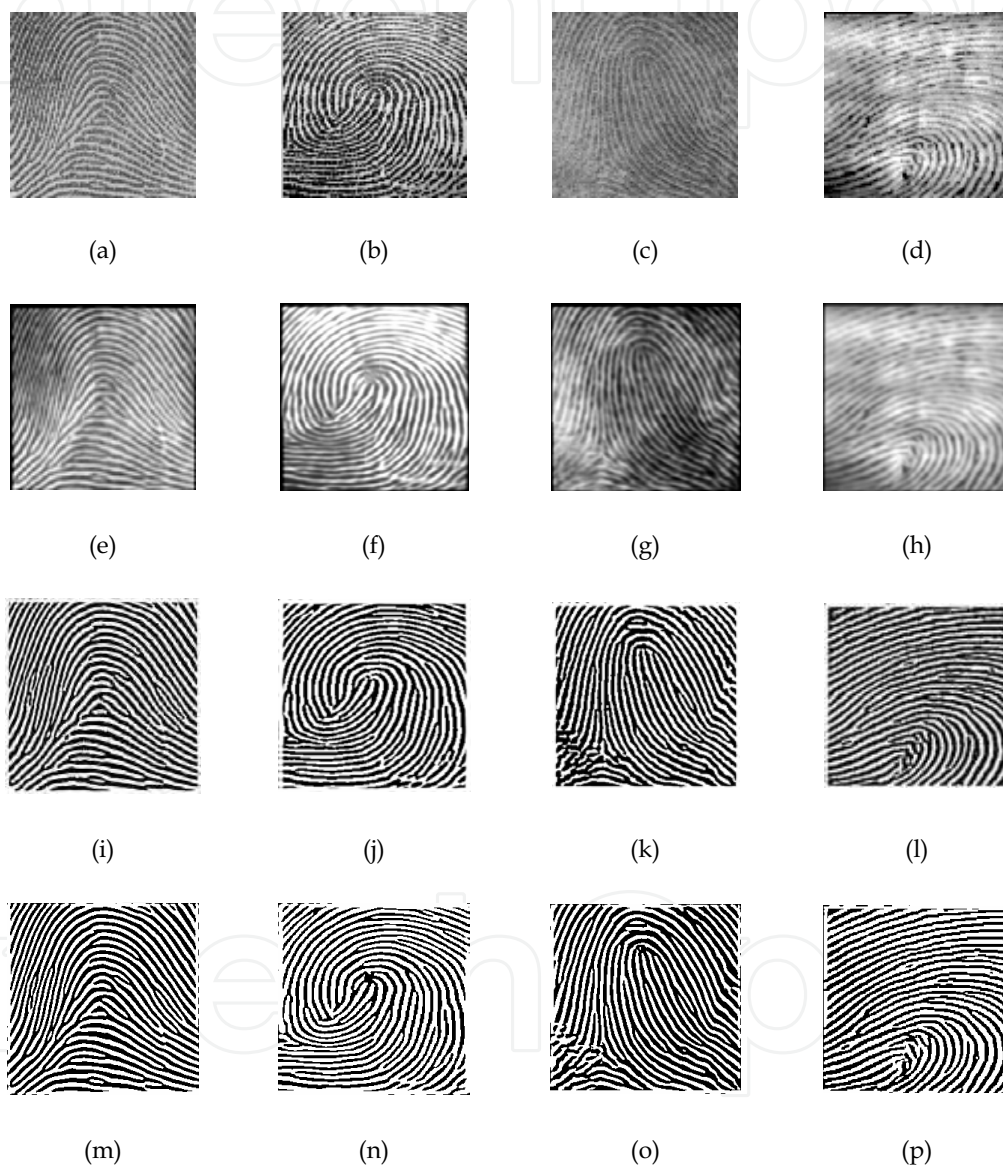

(a)   (b)   (c)   (d)

(e)   (f)   (g)   (h)

(i)   (j)   (k)   (l)

(m)   (n)   (o)   (p)

Fig. 10. Enhancement results of applying different filters to fingerprint images from the same sample set: (a)-(d) original fingerprint images and after enhancement using (e)-(h) the structure-adaptive anisotropic filter, (i)-(l) the proposed unique structure-adaptive anisotropic filter and (m)-(p) the improved Gabor-based filter, accordingly.

Table 1 shows the wall time for different stages of the Gabor-based enhancement algorithm simulated by Hong (1998) and the total time on a Pentium 200MHz PC. The enhancement algorithm based on the anisotropic filter does not require the estimation of the local ridge frequency information. Therefore it saves about 4% of the processing effort compared to the Gabor-based enhancement algorithm.

Normalization (Seconds)	Orientation (Seconds)	Frequency (Seconds)	Region Mask (Seconds)	Filtering (Seconds)	Total (Seconds)
0.11	0.14	0.09	0.07	2.08	2.49

Table 1. The wall time of the Gabor-based enhancement algorithm on a Pentium 200MHZ PC (taken from (Hong, 1998), Table 2)

6. References

Mastin, G.A. (1985). Adaptive filters for digital image noise smoothing: an evaluation, *Computer Vision, Graphics and Image Processing*, No. 31, 103-121.

Donahue, M.J. & Rokhlin, I. (1993). On the Use of Level Curves in Image Analysis, *Image Understanding*, No. 57, 185-203.

Yang, G.Z., Burger, P., Firmin, D.N. & Underwood, S.R. (1996). Structure adaptive anisotropic filtering, *Image and Vision Computing*, No. 14, 135-145.

Zucker, A., Lev, S.W. & Rosenfeld, A. (1977). Iterative enhancement of noisy images, *IEEE Trans. Systems, Man and Cybernetics*, No. 7, 435-441.

Wang, D.C., Vagucci, A.H. & Li, C.C. (1981). Gradient inverse weighted smoothing scheme and the evaluation of its performance, *Computer Graphics and Image Processing*, No. 15, 167-181.

Davis, L.S. & Rosenfeld, A. (1978). Noise cleaning by iterated local averaging, *IEEE Trans. Systems, Man and Cybernetics*, No. 8, 705-710.

Blake, A. & Zisserman, A. (1987). In: *Visual Reconstruction*, MIT Press, Cambridge, MA.

Perona, P. & Malik, J. (1990). Scale-space and edge detection using anisotropic diffusion, *IEEE Trans. Pattern Analysis and Machine Intelligence*, Vol. 12, 629-639.

Smolka, B., Plataniotis, K.N., Lukac, R. & Venetsanopoulos, A.N. (2003). On the Forward and Backward Anisotropic Diffusion Framework, *Proceedings of the 2003 IEEE-EURASIP Workshop on Nonlinear Signal and Image Processing*, (NSIP-03) in Grado, Italy.

Almansa, A. & Lindeberg, T. (2000). Fingerprint enhancement by shape adaptation of scale-space operators with automatic scale selection, *IEEE Transactions on Image Processing*, Vol. 9, 2027-42.

Weickert, J. (2001). Applications of nonlinear diffusion in image processing and computer vision, *Acta Mathematica Universitatis Comenianae*, Vol. 70, 33-50.

Freeman, W.T. & Adelson, E.H. (1991). The design and use of steerable filters, *IEEE Transactions On Pattern Analysis and Machine Intelligence*, Vol. 13, 891-906.

Perona, P. (1992). Steerable-scalable kernels for edge detection and junction analysis, *Image and Vision Computing*, Vol. 10, 663-672.

Yu, W., Daniilidis, K. & Sommer, G. (2001). Approximate Orientation Steerability Based on Angular Gaussians, *IEEE Trans. on Image* Processing, Vol. 10, 193-205.

Yang, G.Z., Burger, P., Firmin D.N. & Underwood, S.R. (1996). Structure adaptive anisotropic filtering, *Image and Vision Computing*, Vol. 14, 135-145.

Hong, L., Jain, A.K., Pankanti, S. & Bolle, R. (1996). Fingerprint Enhancement, *Proc. First IEEE WACV*, Sarasota, Fla., 292-207.

Hong, L., Wan, Y. & Jain, A. (1998). Fingerprint Image Enhancement: Algorithm and Performance Evaluation, *IEEE Trans. Pattern Analysis and Machine Intelligence*, Vol. 20, 777-789.

Donahue, M.J. & Rokhlin, S.I. (1993). On the Use of Level Curves in Image Analysis, *Image Understanding*, Vol. 57, 185-203.

Lee, H.C. & Gaensslen, R.E. (1991). *Advanced in Fingerprint Technology*, Ny: Elsevier.

Hollingum, J. (1992). Automated Fingerprint Analysis Offers Fast Verification, *Sensor Review*, Vol. 12, 12-15.

Hong, L., Jain, A.K., Pankanti, S. & Bolle, R. (1996). Fingerprint Enhancement, *Proc. First IEEE WACV*, Sarasota, Fla., 292-207.

O'Gorman, L. & Nickerson, J.V. (1989). An Approach to Fingerprint Filter Design, *Pattern Recognition*, Vol. 22 ,29-38.

Sherlock, D., Monro, D.M. & Millard, K. (1994). Fingerprint Enhancement by Directional Fourier Filtering, *IEE Proc. Visual Imaging Signal Processing*, Vol. 141, 87-94.

Ko, T. (2002). Fingerprint enhancement by spectral analysis techniques, *Proc. 31st Applied Imagery Pattern Recognition Workshop*, pp.133-139.

Huvanandana, S., Malisuwan, S., Santiyanon, J. & Hwang, J.N. (2003). A hybrid system for automatic fingerprint identification, *Proc. 2003 International Symposium on Circuits and Systems (ISCAS'03)*, Vol. 2, 952-955.

Cheng, H., Tian, J. & Zhang, T. (2002). Fingerprint enhancement with dyadic scale-space, *16th Int. Conf. on Pattern Recognition*, Vol. 1, 200–203.

Almansa, A. & Lindeberg, T. (2000). Fingerprint enhancement by shape adaptation of scale-space operators with automatic scale selection, *IEEE Transactions on Image Processing*, Vol. 9, 2027-42.

Wang, S. & Wang, (2004). Fingerprint enhancement in the singular point area, *IEEE Signal Processing Letters*, Vol. 11, 16-19.

Greenberg, S., Aladjem, M., Kogan, D. & Dimitrov, I. (2000). Fingerprint image enhancement using filtering techniques, *15th Int. Conf. on Pattern Recognition*, Barcelona 3, 326-329.

Greenberg, S., Aladjem, M. & Kogan, D. (2002). Fingerprint image enhancement using filtering techniques, *Real-Time Imaging*, Vol. 8, 227-236.

Lee, H.C. & Gaensslen, R.E. (1991). *Advanced in Fingerprint Technology*, Ny: Elsevier.

Vision Systems: Segmentation and Pattern Recognition

Edited by Goro Obinata and Ashish Dutta

Research in computer vision has exponentially increased in the last two decades due to the availability of cheap cameras and fast processors. This increase has also been accompanied by a blurring of the boundaries between the different applications of vision, making it truly interdisciplinary. In this book we have attempted to put together state-of-the-art research and developments in segmentation and pattern recognition. The first nine chapters on segmentation deal with advanced algorithms and models, and various applications of segmentation in robot path planning, human face tracking, etc. The later chapters are devoted to pattern recognition and covers diverse topics ranging from biological image analysis, remote sensing, text recognition, advanced filter design for data analysis, etc.

How to reference

In order to correctly reference this scholarly work, feel free to copy and paste the following:

Shlomo Greenberg and Daniel Kogan (2007). Anisotropic Filtering Techniques applied to Fingerprints, Vision Systems: Segmentation and Pattern Recognition, Goro Obinata and Ashish Dutta (Ed.), ISBN: 978-3-902613-05-9, InTech, Available from:
http://www.intechopen.com/books/vision_systems_segmentation_and_pattern_recognition/anisotropic_filtering_techniques_applied_to_fingerprints

INTECH
open science | open minds